Thermo-conversion of Solid Recovered Fuels under inert and oxidative atmospheres: Gas composition and chlorine distribution

Elias Daouk*, Rababe Sani, Doan Pham Minh, Ange Nzihou

RAPSODEE, CNRS UMR 5203, Mines-Albi, Campus Jarlard, 81013 Albi Cedex 09, France

A B S T R A C T

The interest in thermo-conversion of Solid Recovered Fuels (SRFs) processes for syngas production has increased in the last decades. However, the monitoring and control of trace contaminants in SRFs such as chlorine in syngas still meet difficulties. The aim of this study is to determine the gas composition and to track the chlorine content in the products from the pyrolysis and oxidation of SRFs. Two types of SRFs from two different industrial sites in France were chosen for this study. The first one, SRF1, was chosen for its low chlorine content (0.3 wt% of Cl) comparing with the second one, SRF2 (1.1 wt% of Cl). SRF1 with low chlorine content showed that the most of Cl was transferred into the gas phase during thermo-conversion process. SRF2 with high chlorine content showed more NaCl in the residual solids after the reactions than its initial inorganic chlorine content.

Keywords:
SRF
Thermo-conversion
Gas composition
Chlorine distribution

1. Introduction

In 2012, the EU-28 generated 2 414.4 million tonnes of non-hazardous waste and 100.7 million tonnes of hazardous waste. Germany, France and the United Kingdom made up a 39% share of total EU-28 waste generation. More than 45% of the waste treated was subject to recovery, other than energy recovery, and almost half, more than 48%, was subject to disposal operations other than incineration, mostly landfilling [1].

The EU aims to minimize disposal methods that do not contribute to a valorisation of MSW such as landfilling. Thus, a waste recovery option that offers business opportunities for the waste management companies is to produce the so-called Solid Recovered Fuels (SRF). Referring to the standard EN 15357 [2], Solid Recovered Fuels or SRFs are “solid fuels prepared from non-hazardous waste to be utilised for energy recovery in incineration or co-incineration plants and meeting the classification and specification requirements laid down in EN 15359” [3]. SRFs offer the opportunity to produce energy from processed fractions of MSW that cannot be recycled, which is an acceptable waste recovery option. In 2012, the remaining waste, that was not recovered nor landfilled, was incinerated with energy recovery (4% of waste) and without energy recovery (2% of waste) [1].

In the case of energy recovery, SRFs can thus contribute to the preservation of natural resources as they can substitute fossils fuels. Another major benefit of SRFs is their biogenic contents of the initial waste stream (wood, paper, cardboard…), a carbon dioxide (CO_2) neutral. This biogenic fraction varies with regions and economics and it can be estimated by the determination of biomass content using the standard EN 15440 [4]. Many studies [5–8] showed that SRFs derived from MSW have a high biogenic fraction (50–70%).

For thermochemical conversion processes (incineration, co-combustion, pyrolysis and gasification), there is a big debate about the best technology dealing with biomass and waste. To answer this question, Life Cycle Assessment (LCA) has been used extensively these last decade to study the environmental loads of thermal Waste-to-Energy (WtE) technologies [14]. LCA makes it possible to compare the different technologies, to choose the most adapted thermo-conversion process based on energy, environment and economy criteria. Arena et al. [15] found that combustion and gasification WtE technologies had sustainable environmental performances, but the combustion unit was better for most of the selected impact categories. In contrary, Consonni and Vigano [16] showed that waste gasification has lower generation of some pollutants comparing to conventional WtE. The energy performances of combustion and gasification were very similar.

The gasification of different wastes, including SRFs, has been studied in detail by other authors [9,10,17,18]. Some of these studies have also investigated the influence of process conditions on syngas quality [10,19,20]. By far, the most case-studies assessed combustion and gasification, while relatively few studies focused on waste pyrolysis. From these few studies, pyrolysis characteristic of SRFs were studied at laboratory scale using a thermogravimetric analyser [21,22] or using a fixed bed reactor [23]. In the both cases, tests were performed in non-isothermal conditions: the SRFs samples were heated from room temperature to a fixed high temperature at a constant heating rate

* Corresponding author.
E-mail address: elias.daouk@mines-albi.fr (E. Daouk).

(between 1 and 20 °C/min). Those researchers have focused on the behaviour of SRFs samples from a pure thermogravimetric point of view which involves weight loss as a function of temperature of the sample. It is observed that the volatiles from plastics generally start to evolve at a higher temperature range (300–500 °C) as compared to those from biomass or coals (200–400 °C) [24]. Considering the product yields, the results showed that both light and heavy liquid fractions increased with the presence of plastic material in the waste [25]. They supposed that the olefinic products from plastics thermal conversion react with some products from the biomass depolymerisation to result in the formation of light liquids.

Nevertheless, due to their nature or preparation method, SRFs can contain high levels of chlorine, sulphur, and heavy metals. For thermal processes, they cause fouling, corrosion of pipes and down-stream units, besides poisoning of catalysts [9]. Referring to EN 15508 [8], the technological criterion for SRFs is chlorine content. The chlorine nature in SRF is dual, organic from chlorinated polymers (e.g., PVC) and inorganic, for instance salts (NaCl and/or KCl) from food waste [6,7,11]. In general, the Cl content should be below 0.5 wt% or 1.0 wt% depending on the application.

Worldwide, in term of polymer consumption, polyvinyl chloride (PVC) is ranked second behind polyethylene [12]. Thus, PVC is omnipresent in SRFs composition and they will affect the thermo-conversion and gas composition. Around a half of the chlorine in municipal solid waste (MSW) comes from PVC, which means a half of the HCl in the combustion gases from MSW incinerators [13]. In addition to the formation of HCl, other forms of chlorine such as chlorides of Na, K, Zn, Pb, Sn, Sb, Fe, and other elements in the gas phase can cause high temperature corrosion of incinerators and reactors. To minimize the costly chlorine-associated problems, it is important to study the chlorine concentration in waste, chlorine species and thermal behaviour of chlorine [11].

In this study, we will focus on the fate of chlorine during SRFs pyrolysis and oxidation in an isothermal furnace. The operational conditions of the isothermal furnace, used in this study, imitate the industrial scale operation conditions. The main objective of this study is to determine gas composition and to track the chlorine content during pyrolysis and oxidation for both SRFs.

2. Materials and methods

2.1. Samples preparation and characterization

Two types of SRFs from two industrial producers in France were chosen for this study. During the preparation of the first one (SRF1), an optical detector was used in order to minimize its chlorine content. The second one (SRF2) was prepared without optical detector, and contains obviously more chlorine than that in the first SRF.

Before the characterization and thermo-conversion tests, the two SRFs samples were dried and ground under 1 mm using a rotary cutting mill equipped with a 1 mm sieve (Fig. 1).

The proximate analyses of the two SRFs were carried out according to the EN 15402 [26] for volatile matter and EN 15403 [27] for ash content. The fixed carbon was deduced by difference.

The elemental composition of the samples was carried out according to:

- EN 15407 [28] for the determination of carbon (C), hydrogen (H) and nitrogen (N) content, with a CHN analyser Flash 2000.
- EN 15408 [29] for Sulphur (S) and chlorine (Cl) content. This method consists of an oxygen combustion procedure of the sample in a bomb. Sulphur and chlorine compounds are converted respectively to chloride and sulphate which are absorbed and dissolved in an absorption solution (KOH 0.2 ml/l solution). After each sample's combustion in the calorimetric bomb IKA C500, the bomb was washed out to recover the solution, which were subsequently analysed by ionic chromatography to determine S and Cl contents.
- EN 15410 [30] for the determination of the content of major and trace elements. The method consists of using an inductively coupled plasma-optical emission spectrometer (ICP-OES). Before analysis, the SRFs samples were digested at 220 °C with an adapted acid mixture using a special closed reactor. The dissolution conditions were optimized to dissolve completely these SRFs samples. The most adapted acid mixture was: sulfuric (3 ml), nitric (3 ml), hydrofluoric (1 ml) and hydrogen peroxide (3 ml), with a SRF sample of about 200 mg.

The calorific value was measured following the standard EN 15400 [31], using the calorimetric bomb IKA C500.

Table 1 depicts the results for the characterization of the two SRFs samples. The data of the proximate analysis, C, H, N, O, S, Cl and the LHV are the average of at least triplicate analyses, and the data for the other major and trace elements are the average of at least 5 analyses.



Fig. 1. Illustration of SRF sample for laboratory analysis and experiments.

Table 1
Proximate and ultimate analyses of of SRF1 and SRF2.

Parameters		SRF 1	SRF 2
Moisture content (wt%, w.b.)		7.3 ± 0.2	8.3 ± 0.2
Proximate analysis (wt%, d.b.)	Volatiles	73.3 ± 0.1	74.8 ± 0.5
	Fixed carbon*	9.4 ± 0.3	7.5 ± 0.7
	Ash	17.3 ± 0.3	17.7 ± 0.2
Elemental composition (wt%, d.b.)	C	46.20 ± 0.82	49.90 ± 0.67
	H	6.20 ± 0.42	6.63 ± 0.35
	N	0.60 ± 0.04	0.66 ± 0.01
	S	0.10 ± 0.02	0.51 ± 0.10
	Cl	0.30 ± 0.20	1.09 ± 0.15
	Al	0.99 ± 0.51	0.18 ± 0.05
	Ca	3.35 ± 0.59	1.14 ± 0.37
	Fe	0.24 ± 0.06	0.18 ± 0.01
	K	0.14 ± 0.06	0.12 ± 0.03
	Mg	0.22 ± 0.10	0.21 ± 0.01
	Na	0.46 ± 0.01	0.47 ± 0.01
	P	0.15 ± 0.02	0.09 ± 0.04
	Si	1.00 ± 0.03	1.19 ± 0.11
	Sn	0.08 ± 0.02	0.10 ± 0.01
	Ti	0.14 ± 0.01	0.24 ± 0.06
	Zn	0.03 ± 0.01	0.23 ± 0.07
Trace elements (mg/kg, d.b.)	As	39.0 ± 23.3	26.1 ± 14.0
	Cd	13.6 ± 10.6	5.6 ± 1.4
	Co	9.2 ± 6.4	10.2 ± 8.0
	Cr	77.0 ± 5.8	126.4 ± 19.8
	Cu	45.0 ± 10.8	610.2 ± 105.6
	Mn	78.4 ± 5.4	97.5 ± 48.8
	Ni	46.7 ± 30.4	49 ± 11.6
	Pb	27.7 ± 30.9	1.4 ± 1.2
	Sb	45.7 ± 7.1	28.8 ± 4.8
	Tl	1.0 ± 8.7	1.5 ± 0.5
	V	28.9 ± 3.5	89.1 ± 12.6
	Hg	0.10 ± 0.01	0.74 ± 0.03
LHV (MJ/kg, d.b.)		23.2 ± 0.2	22.6 ± 0.3

* By difference; w.b.: wet basis, d.b.: dry basis.

The proximate analysis shows that the volatile matters content of the SRF2 is slightly higher than that of SRF1. The ash content was high for both SRFs and reached more than 17%. Finally, the fixed carbon of these two SRF samples accounts for 9.4 and 7.5 wt%, respectively and is in accordance with the literature data [22]. The very low content of the fixed carbon measured in this work is commonly found for this kind of SRFs, which mainly are composed of plastics, refused paper and biomass. According to elemental analysis, there was no notable difference between the two SRFs except for chlorine content and some other elements (i.e. C, S, Ca, Al, and Zn). The chlorine content of these SRFs (0.30 ± 0.20 for SRF1 and 1.09 ± 0.15 for SRF2) confirmed the effect of PVC elimination step during their preparation. Knowing that plastic materials present the highest elemental carbon content (63–91 wt%) among the SRFs samples [22], this could explain the highest C content observed for SRF2 (49.9 wt%) in comparison with SRF1 (46.2 wt%). The higher plastics content in SRF2 comparing to SRF1 can explain the slightly higher amount of H observed in SRF2.

2.2. Chlorine content in SRFs

2.2.1. Total chlorine

One of the parameters to assess the thermo-conversion performance is the tracking of the evolution of chlorine from the SRF to the products (solid residue and gas). This paragraph is dedicated to detail the method adapted and used in this study to measure the chlorine content in SRF and solid residue (char and ash) after thermo-conversion process.

As mentioned previously, the method used for chlorine determination is based on the standard EN 15408 [29]. This method consists of an oxidation of the sample in a calorimetric bomb followed by the analysis of the resulting solution in an ionic chromatography. In order to check the reliability and to validate our method of determination of chlorine content in the SRFs, a control test was carried out. For this purpose, a model sample consisting of a mixture of wood with a well-known content of polyvinyl chloride (PVC) was used. The average recovery for chlorine from the calorimetric bomb to the solution for ionic chromatography analysis was around 94%. This value is in the range recommended by the standard EN 15408 [29], which allows validating the analysis method.

2.2.2. Organic and inorganic chlorine

The total chlorine content in the SRFs can be separated into two main categories:

- Organic chlorine from plastics, mainly PVC;
- Inorganic chlorine from salts, mainly kitchen and garden wastes.

Organic and inorganic chlorine have a distinctly different thermal behaviour. It is important to quantify the proportion of each chlorine type in SRFs in order to understand and to track their evolutions during thermo-conversion tests. For this purpose, an elution test was used which provides the possibility to distinguish organic and inorganic chlorine [11]. Fig. 2 shows the steps of the elution procedure used in this study to determine the inorganic and organic chlorine contents in SRFs. This method is based on the fact that, for SRFs, water-soluble chlorine is referred to as inorganic chlorine and non-water-soluble chlorine, which remains in the solute after elution, is referred to as organic chlorine.

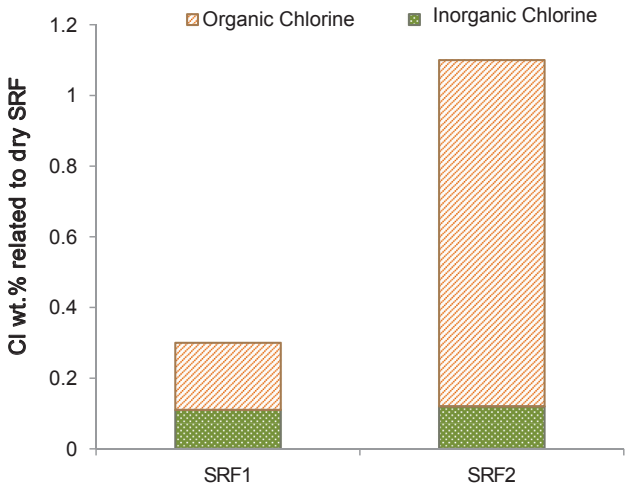


Fig. 3. Chlorine content and its distribution between organic and inorganic chlorine for both studied SRFs.

Fig. 3 shows the results of chlorine content of both SRFs studied in this study (SRF1 and SRF2), and the distribution of organic and inorganic chlorine for each SRF from the elution method. The amount of inorganic chlorine was similar for both SRFs (about 0.12 wt%). On the other hand, the organic chlorine fraction was much higher for SRF2 (0.98 wt%) than for SRF1 (0.19 wt%). In fact, for the SRF1, PVC, which was the main organic chlorine source, was mostly eliminated during its preparation by an optical detector as mentioned above.

2.3. Experimental device and procedure

Fig. 4 shows the experimental setup used to study SRFs pyrolysis and oxidation under isothermal conditions. It is mainly composed of a reactor tube (20 mm internal diameter) made by inert ceramic and heated by an electrical furnace, and a gas trap system.

Thermo-conversion experiments were performed under both inert atmosphere of nitrogen, and oxidant atmosphere of air. The experiments were carried out with a fixed inlet gas flow rate of 200 ml/min, under isothermal conditions. After heating the reactor to the desired temperature (800 °C), the inert crucible with the SRF sample (700–800 mg) was rapidly introduced in the reactor, for less than 15 s to start the thermos-conversion process. The temperature evolution around the sample was measured, and we observed that the heating

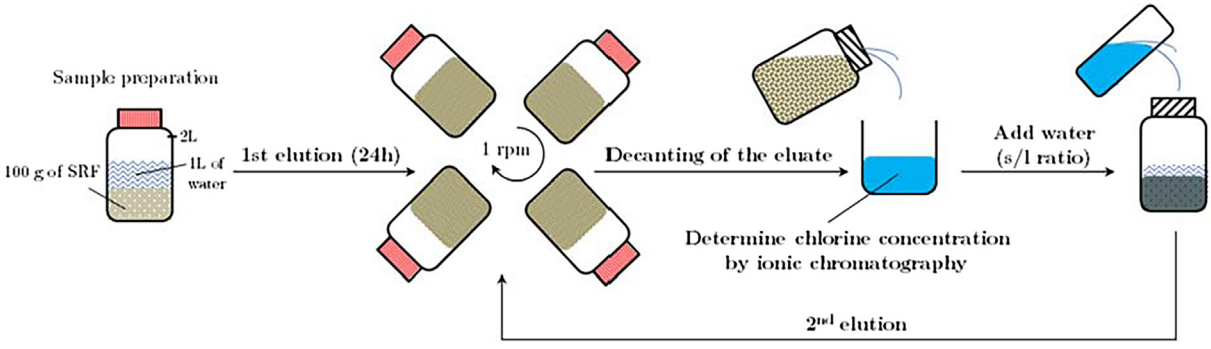


Fig. 2. Elution procedure for the determination of organic and inorganic chlorine contents.

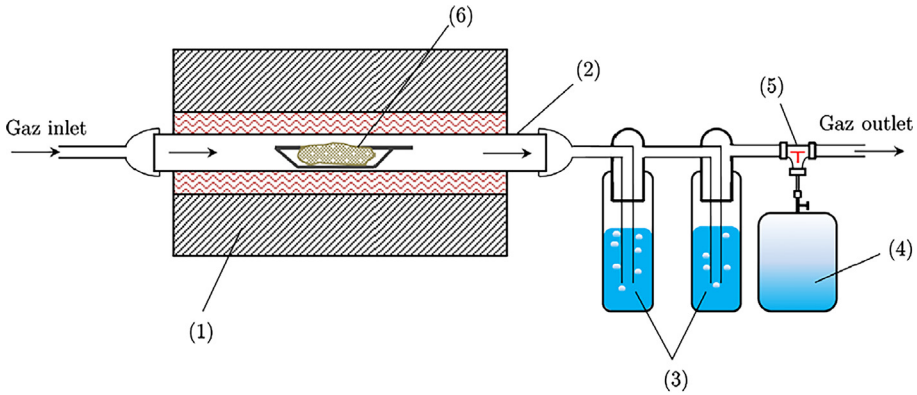


Fig. 4. Diagram of experimental device. (1) Furnace; (2) reactor; (3) isopropyl alcohol impengers; (4) gas sampling bag; (5) three-way valve; (6) crucible with SRF sample.

rate at the beginning is around 1600 °C/min from room temperature up to 520 °C, after the hating rate is around 80 °C/min up to 730 °C, and finally we measured 20 °C/min from 730 °C up to 795 °C.

At the outlet of the reactor, the produced gas passes through a series of condensers containing isopropyl alcohol in order to remove particulates and condense water and tars. After, the permanent gas is recovered along the test, during 20 min, in a sampling bag for subsequent analyses. Each test was repeated at least threefold.

A micro-GC (MyGC Agilent) was used to quantify the major components in the permanent gas (H_2, O_2, N_2, CO, CO_2, CH_4, C_2 and C_3) recovered in the sampling-bag. Nitrogen, which is an inert gas, was used as internal standard to calculate the total mass of permanent gas (m_{PG}), from the sample, at reactor output according to Eq. (1):

$$m_{PG} = \frac{m_{N_2,i}}{Y_{N_2,o}}(1-Y_{N_2,o}-Y_{O_2,o}) \quad (1)$$

where $m_{N_2,i}$ is the mass of introduced nitrogen during the 20 min of recovering gas in the sampling-bag. $Y_{N_2,o}$ and $Y_{O_2,o}$ are respectively the nitrogen and oxygen mass fractions in the gas recovered in the bag (calculated using the micro-GC results). The mass of condensates (tars, particulates and water) was deduced taking into account the mass of permanent gases and the mass of the solid fraction that remained in the reactor. In the case of pyrolysis, the sum of the products is equal to the SRF sample mass. In the case of oxidation, a part of the oxygen from the introduced air reacts with the SRF sample. Thus, the total mass of all the products is calculated from the mass of SRF sample and the oxygen consumed during the reaction.

The residual solid product after test (char after pyrolysis test or ash after oxidation test) was collected and analysed to measure its chlorine content. For chars, the method based on the standard EN 15408 [29] was directly used. Because ashes are of an incombustible nature, a mixture of wood and ash was prepared. Then, the standard EN 15408 [29] was applied for this mixture to measure its chlorine content. The crystalline structure of Cl containing compounds in the produced chars or ashes was also analysed by X-ray Diffraction (XRD, PanAnalytical X'PertPhilips). XRD patterns were analysed by using software X4Pert HighScore based on ICDD database.

2.4. Thermodynamic equilibrium model

In order to develop an idea on the distribution and forms of chlorine in both gaseous and solid phases under the thermos-conversion conditions used, thermodynamic equilibrium calculations were carried out using FactSage.

FactSage is a thermodynamic program developed by Thermfact in Canada and GTT-Technologies in Germany, and it is one of the largest fully integrated database computing systems in chemical thermodynamics. Equilibrium calculations use the Gibbs energy minimization method at fixed temperature and pressure. In our case, the pressure was fixed at 1 atmosphere and the temperature was varied from 500 to 800 °C.

3. Results and discussion

3.1. SRFs pyrolysis

3.1.1. Product yields and permanent gas composition

Fig. 5 shows the permanent gas, char and condensable yields obtained from pyrolysis experiments of both SRFs at 800 °C. For each experiment, the product yields were calculated as the percentage of mass of compound per mass of dried SRF sample. The results show the similar char yield (22–23 wt%) for both SRFs. The permanent gas yield was slightly higher for SRF2 (51 wt%) compared to SRF1 (45 wt%), and the condensable yield was slightly lower for SRF2 (27 wt%) compared to SRF1 (32 wt%). These differences presumably derived from the feedstock composition and/or can be related to some tar cracking toward permanent gas products for SRF2.

The permanent gas compositions for both SRFs pyrolysis are presented in Fig. 6. In general, despite the feedstocks differences, the permanent gas composition varies slightly. The major gases were always CO (30–33%vol.) followed by H_2 (16–18%vol.), CO_2 (12–19% vol.), CH_4 (13–16%vol.) and C_2H_4 (11–18%vol.). Some traces of light hydrocarbons (C_3, C_2H_6 and C_2H_2) were also detected. The volume ratio of H_2/CO was close to 0.54 for both SRFs. Considering the volume ratio of CO/CO_2, we observed that it was higher for SRF2 (2.5) than for SRF1 (1.74). This trend can be related to the more intense cracking of the hydrocarbons present in the gas during SRF2 pyrolysis as mentioned

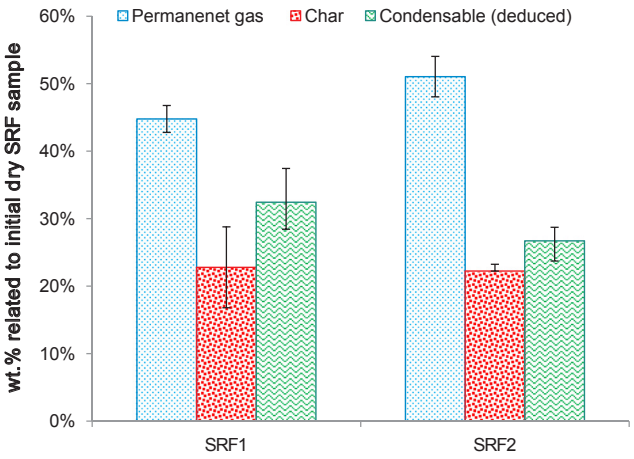


Fig. 5. Product yields of SRFs pyrolysis.

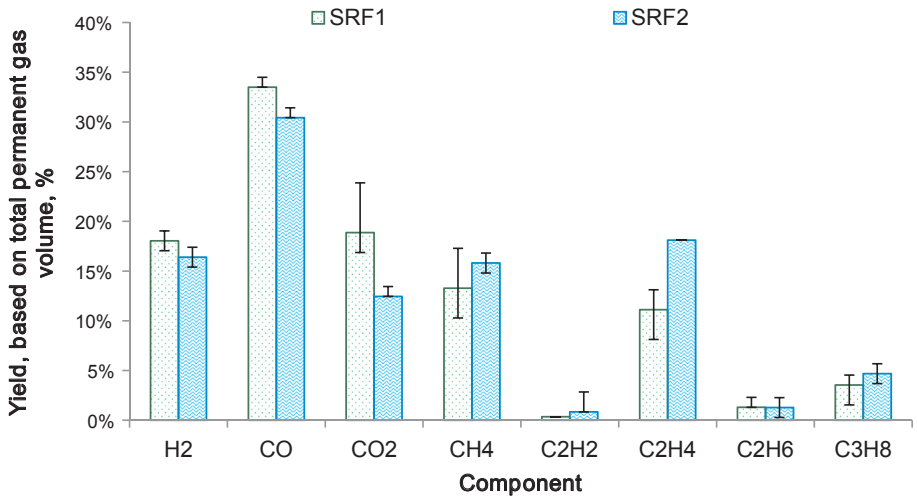


Fig. 6. Permanent gas composition of SRFs pyrolysis.

above [32–34].

The monomer forming the polyethylene plastic PE, ethylene (C_2H_4) is an indicator of PE thermal degradation [24]. This can explain the relatively high percentage of ethylene in the permanent gas produced by both SRFs pyrolysis. Fig. 6 shows that the ethylene is higher for SRF2 compared to SRF1. This result cannot be related directly and only to the amount of PE in the feedstock. In fact, Ahmed et al. [24] showed that blends of PE with another matter, as woodchips (WC), always yielded higher values of hydrocarbons and ethylene compared to PE alone. This indicates the synergic interaction effect between PE and WC, or other components, during the thermal degradation. The presence of acetylene (C_2H_2) in the gas for SRF2, but not for SRF1, can be attributed to the thermal decomposition of PVC as shown in Eq. (2). PVC was much more present in SRF2 than in SRF1.

$$(CH_2CHCl)_n \rightarrow nHCl + nC_2H_2 \quad (2)$$

3.1.2. Chlorine distribution

Fig. 7 shows the chlorine distribution between the gas phase (volatile chlorine) and the solid residual phase (non-volatile chlorine) after the pyrolysis test at 800 °C for both SRFs. We observe that the distinction between inorganic and organic chlorine (Fig. 3) does not correlate with the differentiation between volatile and non-volatile chlorine after pyrolysis (Fig. 7). For SRF1, the majority of the chlorine, around 0.22 wt%, was transferred into the gas phase, and only 0.08 wt % remained in the solid phase. For SRF2, the majority of chlorine was transferred to the gas phase (0.69 wt%), but in this case an important part of the chlorine, nearly 0.41 wt%, remained in the char. For SRF2, the amount of non-volatile chlorine is much higher than inorganic chlorine initially present in the sample (0.12 wt%).

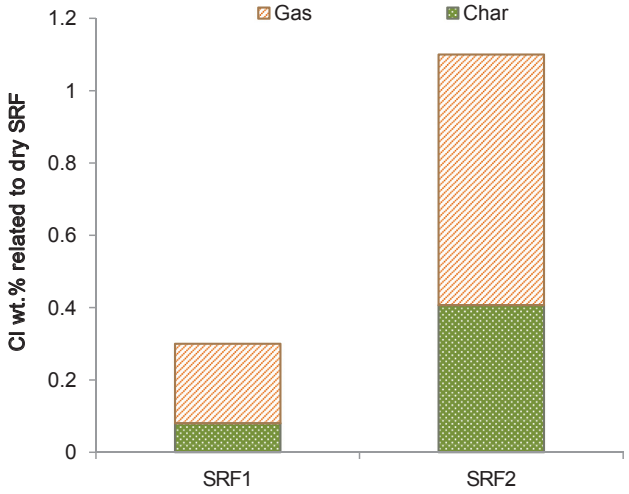


Fig. 7. Distribution of chlorine between the gas phase and the solid residual phase after the pyrolysis tests at 800 °C of both SRFs.

In order to understand and to track the chlorine distribution between the gas and solid phases, the elemental composition of the two SRFs studied (Table 1) was inputted in the thermodynamic equilibrium calculations using FactSage software. The results of the thermodynamic calculations are shown in Fig. 8. The result showed that the chlorine content of the fuels has a significant influence on the production of gaseous HCl, KCl, NaCl, Na_2Cl_2 and K_2Cl_2, and of the solid phases of NaCl and KCl. This result is in a good agreement with the literature [35]. In the case of SRF1, below 700 °C, chlorine exists totally in the solid phase as NaCl and KCl. Above 700 °C the solid phase starts to decrease sharply, leading in high NaCl, KCl, Na_2Cl_2 and K_2Cl_2 in the gas phase. The thermodynamic calculation shows that at 800 °C all the chlorine is transferred to the gaseous phase.

In the case of SRF2, below 700 °C, about a half of the chlorine is transferred into the gaseous phase as HCl and other half remains in the solid phase mainly as NaCl and a small part as KCl. Above 700 °C, solid chlorine compounds start to volatilize sharply leading to higher ratio of vaporised chlorides including NaCl, Na_2Cl_2 and KCl. HCl remains constant in the range of temperatures between 500 and 800 °C for SRF2. So, according to the thermodynamic calculation, chlorine in the initial SRFs can be released to the gas phase under the form of HCl and inorganic salts of Na, K and Ca which are the main inorganic elements of both SRFs.

In order to confirm the results of the thermodynamic calculation, Fig. 9 reports the XRD patterns for both chars produced after pyrolysis tests of SRFs. The presence of the crystalline structure of NaCl in both pyrolysis chars was confirmed, as predicted by the thermodynamic calculation above. The absence of other crystalline phases of Cl containing compounds such as KCl could be due to their low content below the detection limit of XRD, which are in line with the results in Fig. 8 by the thermodynamic calculation. Other crystalline phases were also observed. SiO_2 was commonly found in both chars. On the other hand, $Ca(OH)_2$ and $Ca_3Al_2O_6$ were found only with the char from SRF1, while $CaTiO_3$ was only found with the char from SRF2. These results could be explained by the elemental analysis with high contents of Ca and Al in SRF1, and high content of Ti in SRF2 (Table 1).

From these results, it is highly recommended to eliminate chlorine, in particular organic chlorine (PVC), during SRF preparation before thermo-conversion processes. It appears to be simpler and cheaper to

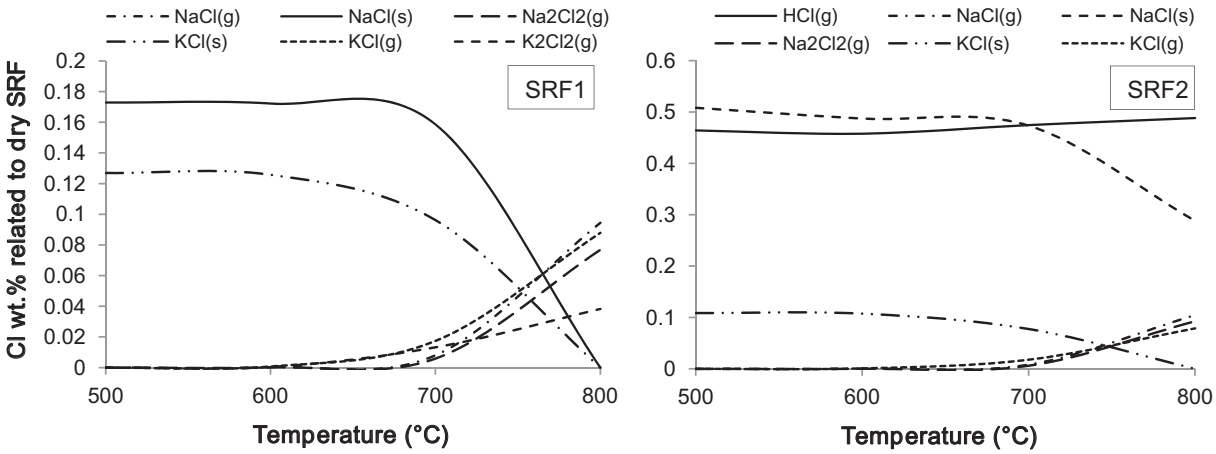


Fig. 8. Percentage of HCl, NaCl, KCl, Na_2Cl_2 and K_2Cl_2 based on dry SRF in both gaseous and solid phases calculated with FactSage.

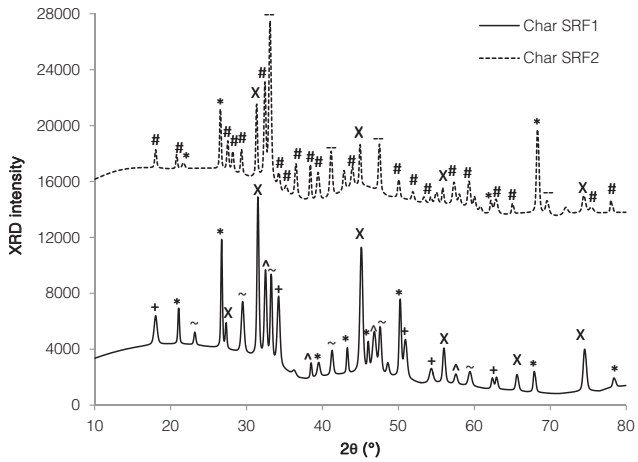


Fig. 9. XRD patterns for both chars produced after pyrolysis tests of SRFs. (x): diffraction peaks of NaCl, (+) diffraction peaks of $Ca(OH)_2$ et (*): diffraction peaks of SiO_2, (~): diffraction peaks of $Ca_3Al_2O_6$, (#): diffraction peaks of Ca_2SiO_4, (^): diffraction peaks of K_2MgSiO_4, and (–): diffraction peaks of $CaTiO_3$.

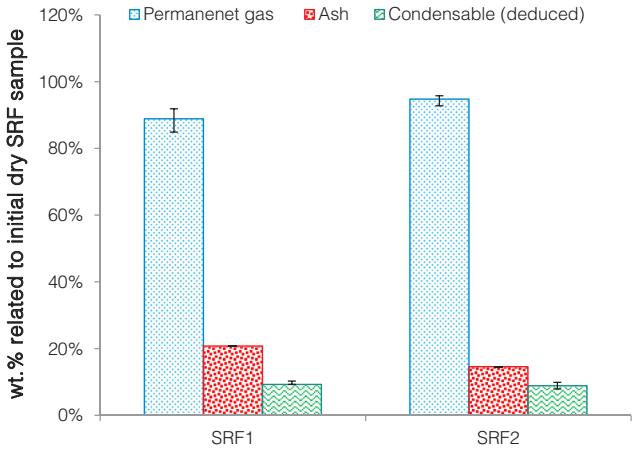


Fig. 10. Product yields of SRFs oxidation.

manage PVC eliminated from SRF preparation than to treat volatile chlorine compounds in the gas phase.

3.2. SRFs oxidation

3.2.1. Product yields and permanent gas composition

Fig. 10 shows the permanent gas, char and condensable yields obtained from oxidation experiments for both SRFs at 800 °C. As a result of using the mass of dry SRF sample basis, the sum of permanent gas, condensable and ash yields was higher than 100%. This is explained by the reaction of O_2 with SRFs components. The mass ratio of O_2/SRF for consumed oxygen during the reaction is defined according to Eq. (3).

$$\frac{O_2}{SRF} = \frac{m_{O_{2,i}} - m_{O_{2,o}}}{m_{SRF}} \quad (3)$$

where $m_{O_{2,i}}$ is the mass of introduced oxygen during the 20 min of recovering gas in the sampling-bag, $m_{O_{2,o}}$ is the mass of oxygen in recovered in the sapling-bag. The same mass ratio O_2/SRF of 0.19 was obtained for both SRFs. The results showed the similar product yields for both SRFs during oxidation. Exactly the same condensable yield of 9 wt% was obtained. The ash yield was higher for SRF1 (21 wt%) compared to SRF2 (15 wt%), leading to a higher permanent gas yield for SRF2 (95 wt%) compared to SRF1 (89 wt%).

The permanent gas compositions for both SRFs oxidation are presented in Fig. 11. Under oxidation atmosphere, the permanent gas compositions for both SRFs were nearly similar. CO_2 represents the majority of the permanent gas (45–50%vol. of permanent gas) followed by CO (18–22%vol.). Despite the oxidation atmosphere, high concentration of CO was observed which could be explained by the short residence time, less than 10 s, of the gas phase inside the reactor. Other permanents gases including C_2H_4 (8–13%vol.), CH_4 (8–12%vol.) and H_2 (5–7%vol.) were also observed even under oxidation conditions.

3.2.2. Chlorine distribution

Fig. 12 shows the chlorine content in the gas phase and the ash after oxidation of the SRFs samples. In the two cases, most of chlorine was transferred into the gas phase as HCl and vaporised metal chlorides. For SRF1, less than 0.06 wt%, remained in the solid phase. This was smaller than the inorganic chlorine content which was originally present in the SRF1 (0.12 wt%). For SRF2, the measured non-volatile chlorine was of 0.17 wt%, which was higher than the inorganic chlorine content originally present in the SRF2 (0.12 wt%). So, the initial organic chlorine in SRF2 was partially remained in the solid fraction.

Thermodynamic calculations under oxidative atmosphere were also performed and the results obtained were similar compared to those under inert atmosphere (Fig. 8). At 800 °C, the calculated yield of chlorine in the solid phase for SRF2 (0.3 wt%) is higher than the experimental measured yield presented in Fig. 12 (0.18 wt%). These differences may be due to the real temperatures during oxidation that can reach values higher than the furnace temperatures, because of the local exothermic reactions. The higher is the temperature, the higher is the chlorine in the gas phase [36].

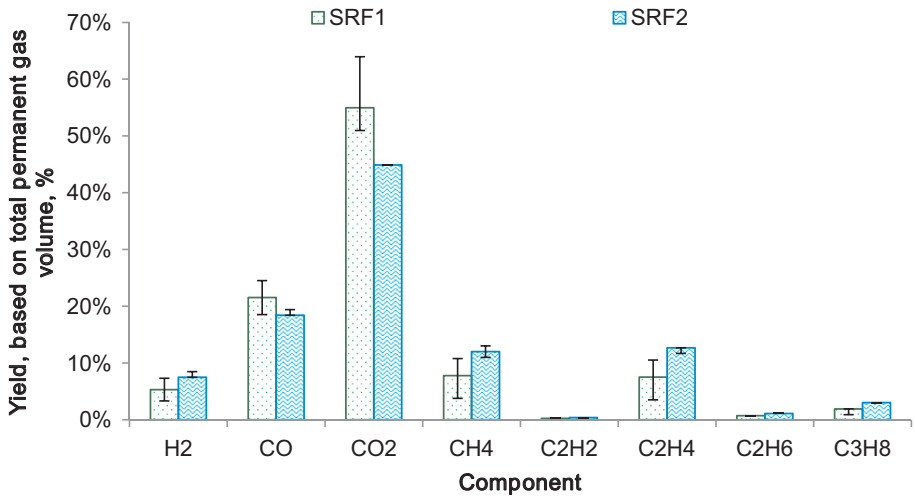


Fig. 11. Permanent gas composition of SRFs oxidation.

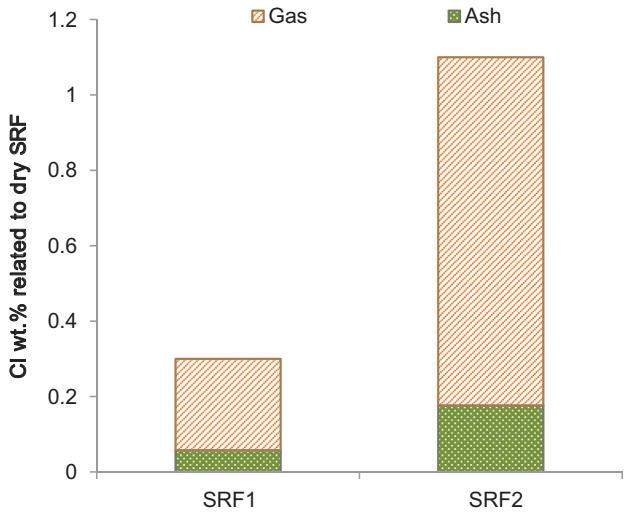


Fig. 12. Distribution of chlorine in the gas phase and the solid residual phase after the oxidation tests at 800 °C of both SRFs.

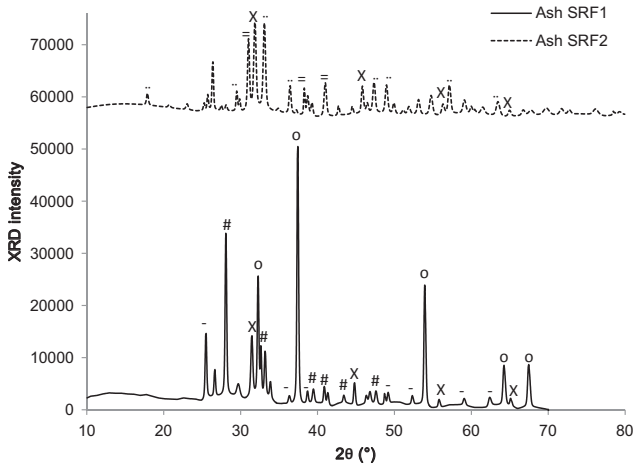


Fig. 13. XRD patterns for both ashes produced after oxidation tests of SRFs. (x): diffraction peaks of NaCl, (¨): diffraction peaks of $Ca_3Fe_2(SiO_4)_3$, (=): diffraction peaks of $FeSi_4P_4$, (o): diffraction peaks of CaO, (#): diffraction peaks of Ca_2SiO_4 and (-): diffraction peaks of $CaSO_4$.

Fig. 13 reports the XRD patterns for both ashes recovered after oxidation tests of SRFs. NaCl was identified as the main chlorinated crystalline compound for both ashes. For the ash of SRF1, a very high peak for CaO was observed. This could be explained by the high Ca content in SRF1 (Table 1) under $CaCO_3$ form which decomposed to form CaO at 800 °C.

4. Conclusion

Thermo-conversion of two different SRFs was performed under inert and oxidative atmosphere in an isothermal furnace at 800 °C. The SRFs were mostly different from their chlorine contents (0.3 wt% for SRF1 and 1.1% for SRF2). The composition of permanent gas was determined and the distribution of chlorine in the products was established.

Under inert atmosphere of nitrogen, the product yields were nearly similar for both SRFs: about 22–23 wt% of char, 27–32 wt% of condensable and 45–51 wt% of permanent gases. The major produced gas were CO (30–33%vol.) followed by H_2 (16–18%vol.), CO_2 (12–19% vol.), CH_4 (13–16%vol.) and C_2H_4 (11–18%vol.). Some traces of C_2 and C_3 were also detected.

Under oxidative atmosphere of the air, both SRFs reacted with the same amount of oxygen during the reaction: the mass ratio of O_2/SRF was around 0.19. The same condensable yield of 9 wt% was obtained for both SRFs. The ash yield was higher for SRF1 (21 wt%) compared to SRF2 (15 wt%), leading to a higher permanent gas yield for SRF2 (95 wt %) compared to SRF1 (89 wt%). CO_2 represented the majority of the permanent gas (45–50%vol.) followed by CO (18–22%vol.), C_2H_4 (8–13%vol.), CH_4 (8–12%vol.) and H_2 (5–7%vol.).

The chlorine initially present in the SRFs was mostly transferred into the gas phase, under inert and oxidative atmospheres, as HCl and vaporised metal chlorides (NaCl, Na_2Cl_2, KCl and K_2Cl_2). Thermodynamic calculations and XRD analysis showed that the crystalline structure of chlorine stacked in the residual solid after reaction was mainly in form of NaCl. In the case of SRF2, with high chlorine content, the amount of non-volatile chlorine was higher than inorganic chlorine initially present in the sample. This indicates that organic chlorine (PVC) partially contributed to the chlorine content of the solid fraction during the thermo-conversion of SRF2. From the results obtained, it is recommended to eliminate chlorine, in particular organic chlorine (PVC), before thermo-conversion processes.

Acknowledgement

The authors thank the technicians at the RAPSODEE centre UMR CNRS 5302 for their technical help. We also thank ADEME for financial

support (PYROG project).

References

[1] Energy, transport and environment indicators – 2015 edition – ESS News display page. http://ec.europa.eu/eurostat/eurostat/web/ess/-/energy-transport-and-environment-indicators-2015-edition.

[2] Solid recovered fuels : terminology, definitions and descriptions: CEN/TS 15357 Technical Specification : English Version. European Committee for Standarization, 2006.

[3] Solid recovered fuels : specification and classes: CEN/TS 15359 Technical Specification : English Version. European Committee for Standarization, 2006.

[4] EN 15440:2011 – Solid recovered fuels. Methods for the determination of biomass content.

[5] Séverin M, Velis CA, Longhurst PJ, Pollard SJT. The biogenic content of process streams from mechanical–biological treatment plants producing solid recovered fuel. Do the manual sorting and selective dissolution determination methods correlate? Waste Manage 2010;30(7):1171–82.

[6] Wagland ST, et al. Comparison of coal/solid recovered fuel (SRF) with coal/refuse derived fuel (RDF) in a fluidised bed reactor. Waste Manage 2011;31(6):1176–83.

[7] Garg A, Smith R, Hill D, Longhurst PJ, Pollard SJT, Simms NJ. An integrated appraisal of energy recovery options in the United Kingdom using solid recovered fuel derived from municipal solid waste. Waste Manage 2009;29(8):2289–97.

[8] Agraniotis M, Nikolopoulos N, Nikolopoulos A, Grammelis P, Kakaras E. Numerical investigation of Solid Recovered Fuels' co-firing with brown coal in large scale boilers – Evaluation of different co-combustion modes. Fuel 2010;89(12):3693–709.

[9] Recari J, Berrueco C, Abelló S, Montané D, Farriol X. Gasification of two solid recovered fuels (SRFs) in a lab-scale fluidized bed reactor: Influence of experimental conditions on process performance and release of HCl, H2S, HCN and NH3. Fuel Process Technol 2016;142:107–14.

[10] Berrueco C, Recari J, Abelló S, Farriol X, Montané D. Experimental investigation of solid recovered fuel (SRF) gasification: effect of temperature and equivalence ratio on process performance and release of minor contaminants. Energy Fuels 2015;29(11):7419–27.

[11] Ma W, Hoffmann G, Schirmer M, Chen G, Rotter VS. Chlorine characterization and thermal behavior in MSW and RDF. J Hazard Mater 2010;1–3(178):489–98.

[12] Scheirs J. Polymer recycling: science, technology and applications. 1 ed. Chichester; New York: Wiley; 1998.

[13] Ma S, Lu J, Gao J. Study of the low temperature pyrolysis of PVC. Energy Fuels 2002;2(16):338–42.

[14] Astrup TF, Tonini D, Turconi R, Boldrin A. Life cycle assessment of thermal Waste-to-Energy technologies: Review and recommendations. Waste Manage 2015;37:104–15.

[15] Arena U, Ardolino F, Di Gregorio F. A life cycle assessment of environmental performances of two combustion- and gasification-based waste-to-energy technologies. Waste Manage 2015;41:60–74.

[16] Consonni S, Viganò F. Waste gasification vs. conventional Waste-To-Energy: A comparative evaluation of two commercial technologies. Waste Manage 2012;32(4):653–66.

[17] Arena U, Di Gregorio F. Gasification of a solid recovered fuel in a pilot scale fluidized bed reactor. Fuel 2014;117(Part A):528–36.

[18] Dunnu G, et al. The solid recovered fuel Stabilat®: Characteristics and fluidised bed gasification tests. Fuel 2012;93:273–83.

[19] Björkman E, Strömberg B. Release of chlorine from biomass at pyrolysis and gasification conditions. Energy Fuels 1997;11(5):1026–32.

[20] Pinto F, et al. Gasification improvement of a poor quality solid recovered fuel (SRF). Effect of using natural minerals and biomass wastes blends. Fuel 2014;117(Part B):1034–44.

[21] Montané D, Abelló S, Farriol X, Berrueco C. Volatilization characteristics of solid recovered fuels (SRFs). Fuel Process Technol 2013;113:90–6.

[22] Grammelis P, Basinas P, Malliopoulou A, Sakellaropoulos G. Pyrolysis kinetics and combustion characteristics of waste recovered fuels. Fuel 2009;88(1):195–205.

[23] Phan AN, Ryu C, Sharifi VN, Swithenbank J. Characterisation of slow pyrolysis products from segregated wastes for energy production. J Anal Appl Pyrolysis 2008;81(1):65–71.

[24] Ahmed II, Nipattummakul N, Gupta AK. Characteristics of syngas from co-gasification of polyethylene and woodchips. Appl Energy 2011;1(88):165–74.

[25] Sharypov VI, et al. Co-pyrolysis of wood biomass and synthetic polymer mixtures. Part I: influence of experimental conditions on the evolution of solids, liquids and gases. J Anal Appl Pyrolysis 2002;1(64):15–28.

[26] EN 15402:2011 – Solid recovered fuels. Determination of the content of volatile matter.

[27] EN 15403:2011 – Solid recovered fuels. Determination of ash content.

[28] EN 15407:2011 – Solid recovered fuels. Methods for the determination of carbon (C), hydrogen (H) and nitrogen (N) content.

[29] EN 15408:2011 – Solid recovered fuels. Methods for the determination of sulphur (S), chlorine (Cl), fluorine (F) and bromine (Br) content.

[30] EN 15410:2011 – Solid recovered fuels. Methods for the determination of the content of major elements (Al, Ca, Fe, K, Mg, Na, P, Si, Ti).

[31] EN 15400:2011 – Solid recovered fuels. Determination of calorific value.

[32] Boroson ML, Howard JB, Longwell JP, Peters WA. Product yields and kinetics from the vapor phase cracking of wood pyrolysis tars. AIChE J 1989;1(3):120–8.

[33] Morf P, Hasler P, Nussbaumer T. Mechanisms and kinetics of homogeneous secondary reactions of tar from continuous pyrolysis of wood chips. Fuel 2002;7(81):843–53.

[34] Rath J, Staudinger G. Cracking reactions of tar from pyrolysis of spruce wood. Fuel 2001;10(80):1379–89.

[35] Dionel O. Albina, Karsten Millrath, N.J. Themelis, Effects of feed composition on boiler corrosion in waste-to-energy plants, 12th North Am. Waste Energy Conf. NAWTEC 12.

[36] Wang Z, Huang H, Li H, Wu C, Chen Y, Li B. HCl formation from RDF pyrolysis and combustion in a spouting-moving bed reactor. Energy Fuels 2002;16(3):608–14.